Biological Forum – An International Journal **15(6): 761-767(2023)**

ISSN No. (Print): 0975-1130
ISSN No. (Online): 2249-3239

Quantitative Measurement and Analysis of Renal Obstruction Using ROI Detection Techniques

Gokhale P.N.[1*], Patil B.R.[2] and Joshi Sameer[3]
[1]Ph.D. Scholar, Department of Electrical Engg., SPCE, Mumbai, (Maharashtra), India.
[2]Principal, VIMEET, (Maharashtra), India.
[3]Director, Miraj Nuclear Medicine and Molecular Imaging Center, (Maharashtra), India.

(Corresponding author: Gokhale P.N.)*
(Received: 30 April 2023; Revised: 27 May 2023; Accepted: 01 June 2023; Published: 10 June 2023)
(Published by Research Trend)

ABSTRACT: We sought to define quantitative measurements of renal radiotracer's density inside the kidneys in terms of renal obstruction levels by applying image processing transforms FFT, Wavelet, and Harr Extraction and find correlation among density measured by transforms and radioactive counts by gamma machine. In this retrospective study, we considered 140 renal scintigraphy scans from which 110 were diagnosed with renal obstruction (hydronephrosis) ranging from moderate to severe and 30 cases were found to be normal functioning kidneys. From 110 cases 64 cases were diagnosed with left kidney hydronephrosis (LK-HL) with M/F ratio of 43/21 and 46 cases were diagnosed with right kidney hydronephrosis (RK-HR) with M/F ratio of 23/23. The mean age of the selected case is 25.65 ± 24.58 years. Three image enhanced transforms namely FFT, Wavelet and Harr Extraction are applied to renal scan to detect the density of darkness inside the kidney. Correlation among density-measured count and scintigraphy-measured radioactive count by Spearman's correlation method. There was strongly positive correlation between FFT measured density inside the kidney and dynamic renal scintigraphy usin^{99m}Tc-DTPA measured radioactive counts in case of both left hydronephrosis kidney and right hydronephrosis kidneys (p=0.81 and p=0.80 respectively). Also found moderately positive correlation among Wavelet and Harr Transform's measures and scintigraphy measures. In conclusion, this study showed that the FFT method can be used to count density in terms of obstruction counts and these quantitative measures of this density can be considered to define the obstruction/hydronephrosis counts instead of reporting moderate level to severe levels.

Keywords: Renal scintigraphy, obstruction, Feature Extraction, Density count, Correlation coefficient.

INTRODUCTION

Renal scintigraphy is a useful medical imaging technique in evaluating the functioning of the kidney. Passive dilation and obstruction of a renal pelvis can be differentiated by using a radioisotope like ^{99m}Tc-DTPA (Diethylenetriamine penta acetate). The renal scintigraphy scan report provides three image panels including perfusion, excretion (drainage of radiotracer), and analysis curve (time activity curve). The time activity curve provides quantitative parameters like radiotracer's peak time, and half time in terms of radiotracer counts per unit of time. With reference to scanning reports, medical experts report the diagnosis in terms of occurrence of renal obstruction/hydronephrosis in the range of moderate level to severe level instead of obstruction count (Gordon *et al*., 2011).

Urinary tract obstacle can arise at any place in the urinary region and is categorized by the level of obstruction. Renal obstruction in the elderly can be due to benign situations such as renal cystic or calculus infection or malignant circumstances such as transitional cell carcinoma of the renal pelvis. Patients with upper urinary tract obstruction of the kidneys or the ureters may face side pain or enlarged tender kidneys. Patients with lower urinary tract obstruction may present with indications of urgency, or incomplete emptying of the bladder (Tseng *et al*., 2009).

Patients going through renal disorders were suggested to go through the renal scintigraphy nuclear imaging test in which medical radioactive isotopes are injected for the evaluation of renal function. Renogram involves sequential imaging after arterial administration of ^{99m}Tc-DTPA. Quantitative assessment of cortical function and collecting system drainage is made using regions-of-interest, that naturally are applied to each kidney. ROI is placed overlying soft tissue neighboring to each kidney. Depending on the ROIs drawn, the time-activity curves (TAC) will replicate the functional accumulation and clearance of radiotracer in the whole kidney, parenchyma, renal collecting system, ureter tube, and bladder (Mititelu and Bratu 2017).

Renal Morphology. Renal hydronephrosis arises when a kidney has an additional of fluid due to no excretion of urine from the kidney and it occurs due to barrier in the upper part of the urinary tract. Urine inside the kidney

increases pressure inside the walls of the kidney and hence renal pelvis gets dilated and swelled.

Bilateral & Unilateral Hydronephrosis. In unilateral hydronephrosis conditions, only one of the kidneys found to be affected while in bilateral hydronephrosis both kidneys are affected. Bilateral hydronephrosis occurs due to incapability of urine is to drain from the kidney into the bladder. The figure 1. Shows stages of hydronephrosis which is defined at the level from stage I to stage II. Stage I indicates the initial stage i.e. mild hydronephrosis. Stage II indicates moderate hydronephrosis while stage III indicates severe hydronephrosis where it's an indication of renal function failure (Andrew *et al.*, 2018).

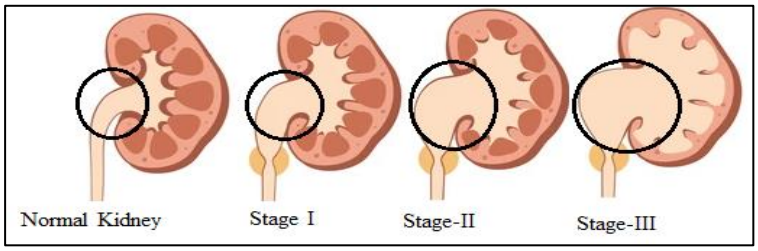

Fig. 1. Stages of Renal Obstruction (Renal Hydronephrosis).

Though the renal scintigraphy procedure indicated the possibility of indication of renal obstruction it doesn't provide any quantitative information which will help the nephrologist to decide the level of obstruction with firm figures. In this study, we focused on counting the density which will provide a direct indication of level of the renal obstruction.

Renogram Components. Renogram as shown in fig.2, is the representation kidney activity curve and blood activity curve.

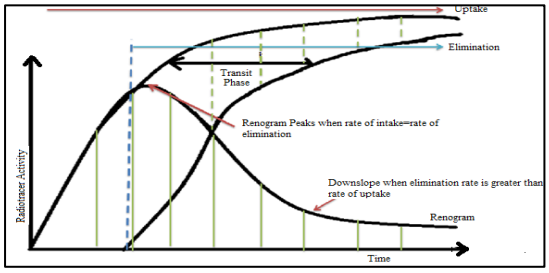

Fig. 2. Renogram Curve.

I: Vascular phase (flow study): It is called as vascular transportation phase, continues for duration of about 30 to 60 seconds

II: Parenchymal phase (kidney to background):-It is the tubular concentration phase of initial parenchymal Transit

III: Washout (excretory) phase: - It is the clearance or excretion phase (Duccio Volterrani, *et al.*, 1990).

Significance of Radioisotope. In this study, renal scintigraphy scans are achieved by using 99m–Technetium Diethylenetriamine pentaacetate (DTPA) radiopharmaceutical. DTPA scan assistances to distinguish uretropelvic junction (UPJ) obstruction from multicycstic kidney and determine the level of obstruction. DTPA is extracted purely by glomerular filtration .means it is excreted unchanged through the kidneys through glomerular filtration, and it is not subject to tubular secretion and /or reabsorption, so its main use is for dynamic real scintigraphy and GFR calculation (Blaufox *et al.*, 2018).

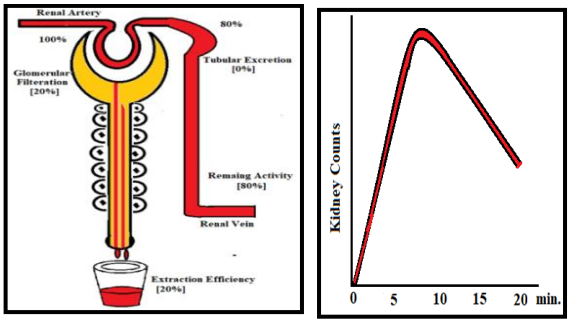

Fig. 3. Glomerular Filtration by DTPA and TAC response.

As shown in Fig. 3. Extraction fraction of radioisotope is around 20%, this extraction fraction is comparatively low related with extraction fraction of tubular renal tracers and hence glomerular filtration rate counted by DTPA is preferred for radioactive excretion count through glomerular.

MATERIALS AND METHODS

The study involved 184 patients' renal scans diagnosed by Siemen's EVO^{TM} model that underwent renal scans between December 1st, 2019, to December 30th, 2021. From 184 cases 140 cases were qualitatively reported as renal obstruction i.e. renal hydronephrosis ranging from moderate to severe levels while 48 cases were excluded from the study due to non-confirmation of renal disorders. From 110 samples 46 were found to be right kidney obstruction and 64 with left kidney hydronephrosis. The mean age of all samples was 25.63±24.58 years. The number of male and female patients for left kidney hydronephrosis cases was 43 and 21, respectively, while for right kidney hydronephrosis cases, it was 23 and 23, respectively. From 140 samples, 30 samples are reported with normal kidney functioning and this data is used for clinical validation comparison with hydronephrosis samples.

Criteria for Sample Selection. Patients aged less than 10 years and those aged more than 65 years were excluded from the study. Renal scans were selected only if they showed gradual tracer accumulation into the dilated pelvis without significant excretion after diuretic

administration. The study did not include cases with horseshoe-shaped kidneys, renal transplants, donors, or single functioning kidneys.

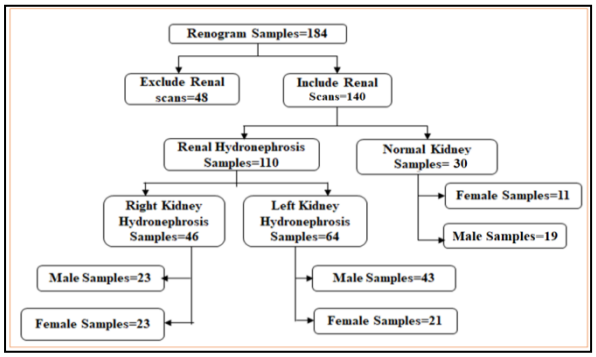

Fig. 4. Sample Classification.

Patient Preparation. All patients were conveyed to drink 500 ml of water and hydrate 20 to 30 minutes earlier radio tracer administration. Patients were asked to void their bladder before the scan procedure. All studies were performed on an XR/T gamma camera attached to a dedicated computer (Siemen's EVO) with low energy all-purpose collimator. The subject is positioned supine, started the acquisition, and then intravenously administered radiopharmaceutical ^{99m}Tc-DTPA as a bolus of 200 MBq (5.4 mCi) (Mititelu and Bratu 2017).

Renal Scan Image Acquisition Process. As shown in figure 4. Renal scintigraphy includes sequential imaging after administration of Tc-99m DTPA. A commonly used technique involves dynamic acquisition of 1 to 2 second images for 1 minute followed by 60 second images for 20 to 30 minutes. Depending on age, gender and weight dose of radiotracer varies. Displayed images correspond to the radioactive bolus passing through aorta to renal arteries in the flow observation, followed by the passage of the radioactivity through the kidneys (ACR Guidelines, 2008).

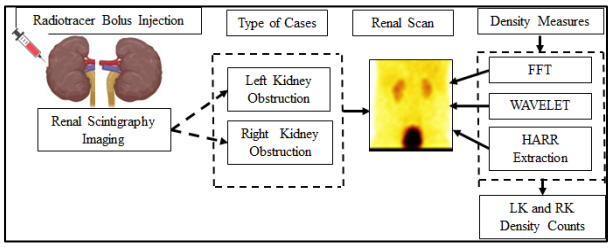

Fig. 5. Renal Scintigraphy Procedure.

Whole-kidney ROI is positioned around the whole kidney, including the renal parenchyma, and relative tracer uptake in each kidney is measured. In obstructive renal disease, the curve generated from the ROI placed on the affected kidney has a distinctive appearance slow continuous accumulation of radiotracer in the collecting system, a slow increasing ascending curve (Filipczak *et al*., 2020). Figure 6 (a) indicates detected right kidney obstruction and 6 (b) scan indicates right kidney obstruction. In both cases time activity curve which is results of ROI drawn region shows peak time of radiotracer uptake but fails to read half time of radiotracer uptake as in both cases respective kidneys were found to be obstructed.

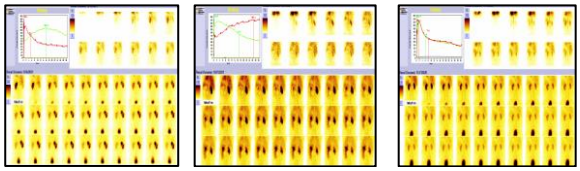

Fig. 6(a). Left kidney (L.K.) Hydronephrosis **6(b)** Right kidney (R.K.) Hydronephrosis Renal Scintigraphy Scan **6(c).** Normal kidney Renal Scintigraphy Scan (NMMIC-SIEMEN's EVO) (NM&MIC).

While, figure 6 (c) represents renal scan of normal functioning kidney whose time activity shows peak time as well as half time of an uptake of radiotracer and ends of both curves are decreasing towards zero which indicates that both kidneys are functioning normally. Hence we are considering only last 30th frame of a complete scan which represents ending status of renal scan acquisition of both the kidneys and represents their response to radiotracer excretion.

Renal Scintigraphy Image Processing. By using suitable color range, a parametric image of each kidney can be gained, allowing the pixel-bypixel true mean transit time in the cortical area and mean transit time (MTT) image can be accommodated in renal image processing easily. Estimation of relative renal uptake of radiotracer and its excretion rate through the kidney can be achieved by using iterative deconvolution and Rutland-Patlak methods in which reported matrix inversion deconvolution values were significantly higher than Rutland-Patlak values (Al-Shakhrah, 2010).

Using adaptive edge based active contour models for kidneys segmentation on dynamic renal scintigraphy which automatically adjusts the rigidity of the snake during its evolution towards an image contour but its clinical use found to be limited for the estimation of glomerular filtration rate and effective plasma renal flow (Suapang *et al.*, 2015).

Initial detection of clinically substantial renal hydronephrosis caused by ureter pelvic junction obstruction was achieved by using automated signal examination and machine learning framework. But as the value of the signal analysis depends extremely on the value of the data obtained by qualified nuclear medicine physicians and technologist's accuracy level of earlier detection of obstructed cases effects (Blum *et al*., 2018). Renal Scintigraphy images are regularly characterized by much noise and low contrast and resolution characteristics while using ^{99m}Tc-DTPA, which observes the regions of interest very complicated and difficult to analyze in terms of diagnosing the level of obstruction i.e. hydronephrosis. Here every digital image is a set of coordinate values "nij" which corresponds to the number of counts in a set of pixels recognized by (i, j). These pixels are signified in matrix form by {(i, j, nij)}.

Drawing the defined region of interest (ROI) around the high density darkened area inside the kidneys and counting the activity on all the selected pixels for P-recorded images, not only allows the tracing over

radioactivity time but also the evolution of the activity of the structure analogous to the selected pixels. Data is then stated in a matrix by introducing the time parameter tk which shows the progress of images: {(i, j, nij), tk} (Jianhua and Yanling 2011).

In this study three image enhancement techniques Wavelet transforms, FFT transform and Harr extraction are applied on each sample and quantify darkness in terms of the density of the last frame of each scan (here in case of SIEMENS gamma scan frame's last 30th image) is measured and these results are clinically validated with the amount measured by Gamma machine's radioactive kidney counts. Thus in this study, following steps are designed and followed to find the best of transform which will approximately match to the clinical report and will provide quantity in terms of density of the obstructed part of the kidney.

Significance of Image enhancement transforms. The density counts measured by three different transform namely FFT, Wavelet, and Harr Extraction indicates the presence of radioactive tracer inside the kidney. In the case of hydronephrosis kidney due to the obstruction tracer remains inside the kidney and cants excrete out of the renal system. In this study, the density of darkness inside the kidney measurement is achieved by enhancing and extracting the kidney structure of renal scan. It is achieved by applying mentioned image processing transforms.

Image feature withdrawal is a transformation procedure in which low the dimensional space of the sample's space is utilized into high dimensional space of an image sample and thus dimension reduction is achieved. Image features are the most fundamental characteristics used to identify an image. The properties of one image can be used to distinguish it from other images. The assignment of the feature extraction using transform algorithms is to extract the image properties which can distinguish this image from others. In the feature extraction techniques, there are four forms of image features often used: gray image features, texture features, shape features, and spatial relationships among pixels.

Table 1: Noble features.

Sr. No.	Feature Types	Characteristic
1	Reliability	The program can designate the features of object in entire.
2	Distinctive ness	Each individual of an object must have its own exclusive representation which can be used to distinguish it from other objects.
3	Quickness	Descriptive methods can easily reflect the differences between similar objects.

Through image feature extraction, features should be able to describe objects abstractly and concretely, so as to provide a reliable basis for subsequent classification. Noble features should have the following characteristics (Patrick, 1990).

Thus, decent features can entirely identify the object (here in the case of darkness inside the kidney) which is required to be identified. In this study, three effective feature extraction methods namely Wavelet Transform, FFT Transform, and Harr Extraction transform are applied to renal scan to extract the features so that the design of classifiers can be precise and more accurate to define the density of darkness.

a) Wavelet Transform

In renal scintigraphy, motion detection is restricted due to the high level of noise and fading of organ boundaries and it represents inherent image characteristics. These restrictions can cause a reduction in the precision of motion detection in cases especially radiotracer's transit process through renal parenchyma to the cortex. The wavelet coding is constructed on the concept that the coefficients of a transform that decorrelates the pixels of an image can be coded more efficiently than the original pixels themselves (Eoran, 1988; Gonzalez, 2001). In this study, direct wavelet transform method with the utilization of the multilevel decomposition of the image is applied and all levels of wavelet decomposition by the analysis of the peak moments of rows and columns coefficients matrixes of the density object were detected. For the object detection we considered two images including templates of an object's image $F = \{f_{i,j}\}$ with $M_1 \times M_2$ $(M_1 = 2^u, M_2 = 2^v, u, v \in Z)$ and common image $A = \{a_{i,j}\}, i = \overline{0, N_1 - 1}, j = \overline{0, N_2 - 1}$ in which this object should be identified. For template image= $\{f_{i,j}\}$, we perform its 'p' levels fast dyadic wavelet transform (p=q,….,0, $q = log_2[min(M1, M2)]$). For kidney detection approximation wavelet coefficients of the image is used because details of coefficients were found to be sensitive to noise influence. The size of matrix of the coefficients for each level doesn't change and hence in this study, shift invariant wavelet transform applied and it is given by:

$A^{P-1}(i,j) = \sum_{K_1=0}^{L-1}(\sum_{K_2=0}^{L-1} A^P(i + 2^{q-p}K_1, j + 2^{q-p}K_2).l_{k_2}).l_{k_1}$---------- (1)

Fig. 7 shows sample application results of left hydronephrosis kidney.

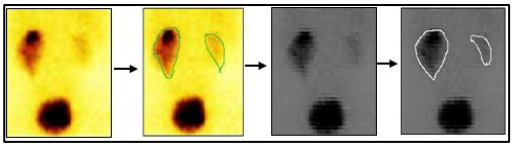

Fig. 7(a). Density count defined ROI using Wavelet Transform.

b) Fast Fourier Transform (FFT)

The Fast Fourier Transform-Low Pass (FFT) is a mathematical field. In this study, FFT-LP is used for renal image filtering, image reestablishment, and image density count measurements. It is a significant image processing tool that is used to decompose an image into its sine and cosine components. While dealing with the derivation of the FFT it is expressed as:

$F(u) = \sum_{X=0}^{M-1} f(x) W_M^{ux}$ …(2)

Where, u=0, 1, 2, M-1, where

$W_{M=e^{-2j\pi/M}}$ …(3)

And M is assumed to be in the form of $M = 2^n$ with 'n' positive integer (Jagtap, 2010). The transformation output represents the image in the frequency domain,

while the input image is the spatial domain equivalent. In the frequency domain image, each point represents a particular frequency contained in the spatial domain image.

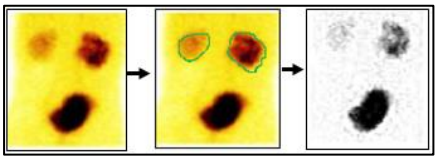

Fig.7 (b). Density count defined ROI using FFT-LP Transform.

c) Harr Extraction. Harr transform can be stated in matrix form which is expressed as:

$$T = HFH^{\tau} \quad \ldots(4)$$

Where, F is an 'N×N' image matrix, H is an, N×N, Harr conversion matrix and T is the resulting N×N transform. In this study this transform is applied on 1100×300 matrix of 1 frames/minute scan of radiotracer excretion of total 30 frames and last 30th frame is focused to count density of darkness inside the kidneys. Also, multi-resolution analysis is achieved by using Harr extraction method and it is achieved by designing an algorithm that will make a rectangular part of a renal scintigraphy frame image and divide that rectangle into multiple parts to count. They are regularly imagined as black and white adjacent rectangles.

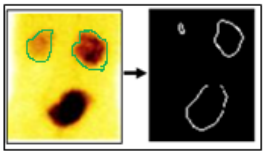

Fig.7(c). Density count defined ROI using Harr Extraction Transform.

The Flowchart of Proposed System

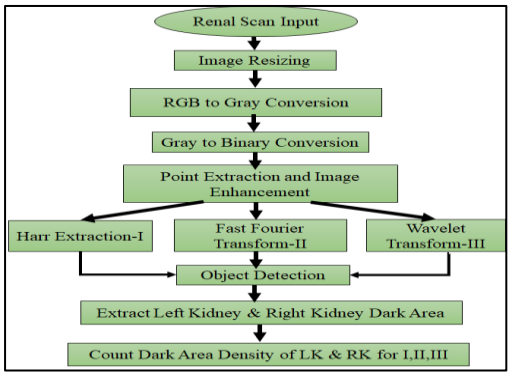

Fig. 8. Flowchart of Proposed Density Count Algorithm.

Steps of Density measurement: Radiotracers half time ($T_{1/2}$) less than 10 minutes indicates that there is no significant obstruction present, values more than 20 minutes are considered to be obstructed kidney**.** Values between 10 minutes to 20 minutes considered to be in determined values of obstruction levels. Renal scan frame samples considered in this study are in the range of 30 frames for 30 minutes i.e. 1 frame/minute. Each frame from first rank to 30th rank is an indication of radiotracer's uptake, renal pelvis's response and excretion from pelvis to cortex, then urinary bladder through urinary tubes**.** As shown in the figure 9 renal scan's 30th image is selected from a matrix 1100×300 of the whole frame of each case of left kidney hydronephrosis, right kidney hydronephrosis and normal functioning cases.

It is converted to RGB to gray in which the saturated information is removed and then gray to binary conversion in which the visual appearance of pixels is increased. Point extraction is performed on each of left kidney and right kidney of all cases. Object detection is achieved by applying the mentioned three image enhancement techniques. The dark area inside the kidney is counted in terms of the density of darkness.

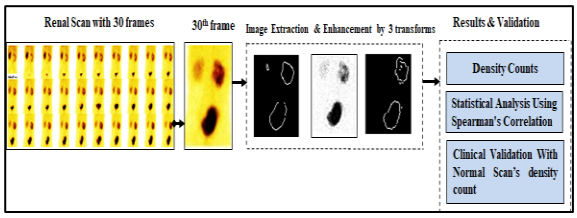

Fig. 9. Methodology Flow Diagram.

RESULTS

Sixty fours patients with left kidney hydronephrosis cases (M/Fe: 43/21) and forty six patients with right kidney hydronephrosis cases (M/Fe: 23/23) were considered in this study. Mean and standard deviation of scintigraphy measured radioactive count.

Table 2: Mean ±S.D. of Radioactive Counts of HL, HR and Normal cases by scintigraphy scan.

Type of Category		Mean Value± S.D.
DTPA HL	LK	66.76±8.25
	RK	33.24±8.25
DTPA HR	LK	36.66±10.44
	RK	65.34±10.44
NORMAL	LK	48.43±4.59
	RK	51.57±4.59

Table 2 and 3 Indicates the mean and the standard deviation values of transforms measured density counts including normal functioning kidney cases.

Findings of Spearman's correlation coefficient values help to understand linear association between two continuous variables. Grading table of Spearman's correlation mentioned in table 3 indicated levels of correlations (positive and negative) among non-parametric data i.e. each transform's measured density count and scintigraphy scan measured radioactive counts (Gokhale and Patil 2022; Mukak, 2012). In this study with reference to the grading ranges mentioned in Table 3. Correlation interpretation is applied.

Table 3. Mean ±S.D. of transforms detected Density Counts of HL, HR and Normal cases.

	FFT	WAVELET	HARR

Type of Category		Mean ± S.D.	Mean ± S.D.	Mean ± S.D.
DTPA HL	LK	68.28±23.11	65.94±22.30	57.06±18.94
	RK	28.59±14.55	27.44±13.76	25.59±13.11
DTPA HR	LK	27.78±18.50	26.87±21.24	22.87±18.50
	RK	70.22±21.22	67.13±20.43	63.43±19.39
NORMAL	LK	19.13±4.92	18.30±4.60	15.63±4.11
	RK	18.50±4.60	17.53±4.43	16.70±4.28

Table 4: Correlation of the transform counts and Scintigraphy counts in case of LK-HL.

Left Kidney Hydronephrosis		
Type of Transforms	Radioactive Counts by Scintigraphy Scan	Correlation Interpretation
FFT	ρ =0.804	Strongly Positive
WAVELET	ρ =0.595	Moderately Positive
HARR	ρ =0.575	Moderately Positive

Table 5: Correlation of the transform counts and Scintigraphy counts in case of RK-HR.

Right Kidney Hydronephrosis		
Type of Transforms	Radioactive Counts by Scintigraphy Scan	Correlation Interpretation
FFT	ρ =0.80	Strongly Positive
WAVELET	ρ =0.57	Moderately Positive
HARR	ρ =0.57	Moderately Positive

DISCUSSION

The standard deviation is a instantaneous quantity of the differences of each observation from the mean and analysis of these observations indicates the location of the center of the data and the standard deviation is the spread in the data. Comparison among mean and standard deviation values derived from three different transforms and renal scintigraphy gamma machines radioactivity counts indicate that:

- In the case of DTPA-HL, density count values derived by FFT transform are more as compared with remaining transforms, as in case of left kidney (68.28±23.11) than right kidney (28.59 ± 14.55) and find to be closer with the radioactive count of the left kidney (66.76±8.25) by scintigraphy machine output.
- Similarly, in case of DTPA-HR, density count values derived by FFT transform is more than the remaining transforms, as in the case of the right kidney (70.22±21.22) than left kidney (27.78±18.50) and found to be closer with the radioactive count of the right kidney (65.34±10.44) counted by the scintigraphy machine .
- In case of the normal functioning kidneys, all three transform density counts are found to be approximately the same as of scintigraphy radioactive counts.

Also in the case of Harr Extraction transform results of the left kidney and the right kidney hydronephrosis were found to be moderately positive i.e. p=0.57 and 0.57 respectively. As shown in the graphical summary

Statistical Analysis for Clinical Validation

Spearman rank correlation is a non-parametric test that is used to measure the degree of association between two variables here in case of finding a correlation among density count measured by image processing transforms and scintigraphy machine detected radioactive counts. A ρ-value of less than 0.05 was considered statistically significant. All statistical analyses were achieved using the SPSS .20 version software. Scan darkness density is measured by three types of image transform techniques namely FFT, Wavelet and Harr Extraction. The table shows correlation in case of the left kidney hydronephrosis cases and the table indicates the correlation rank in case of the right kidney hydronephrosis.

Spearman's correlation coefficient is used to find a correlation between the transform counts results and the scitigraphy's count. We found that, in case of left kidney and right kidney hydronephrosis, there is strongly positive correlation among FFT's density count and scintigraphy radiotracer count i.e. p=0.81 and 0.80 respectively while outputs detected from wavelet transform in case of left kidney and right kidney hydronephrosis found to be moderately positive i.e. p=0.59 and 0.57 respectively.

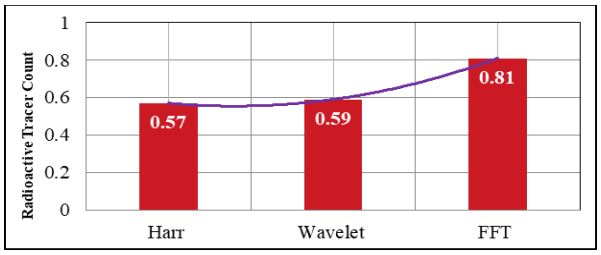

Fig. 10(a) Comparison among Transform Outputs in case of Left Kidney Hydronephrosis.

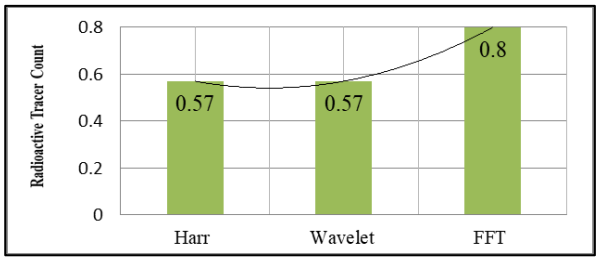

Fig. 10 (b) Comparison among Transform Outputs in case of Right Kidney Hydronephrosis.

analysis, we observed that, out of the three image processing algorithms, the density counts measured by using FFT method are more precise and approximate to scintigraphy detected radioactive counts in both the cases of renal hydronephrosis.

Also results from remaining transforms Wavelet and the Harr Extraction are moderately close to the scintigraphy output.

CONCLUSION

Diagnosis and assessment of renal disorder is achieved by renal scintigraphy method by measuring radioactive counts of absorbed radiotracer. While reporting patient's hydronephrosis level quantitatively medical experts finds limitations using renal scintigraphy procedure as the scintigraphy cannot provide renal obstruction count. In this study we processed renal obstruction (also referred as renal hydronephrosis) scans using image extraction and enhancement processing transforms namely FFT, Wavelet and Harr and measured darkness of radiotracer inside the kidney in terms of density. We found that, density counts measured by FFT are approximately closer to radiotracer radioactive counts measured by scintigraphy machine. Thus, FFT's density count can be considered as a support for diagnosing level of hydronephrosis quantitatively instead of mentioning levels from moderate to severe as these FFT measured density counts found to be directly proportional to radiotracer's counts.

This study will support nephrologist and urologist to define stages of renal hydronephrosis i.e. renal obstruction in terms of count and it will be time saving and cost saving in terms of precise diagnosis, treatment and medication.

FUTURE SCOPES

Addition of various Renal Abnormalities:

Similar to this study, a quantitative measurement technique can be applied to different renal disorders including tumors, cysts, calculi, etc. which could help in the assessment of the patient's diagnosis and medication plan.

Acknowledgement. We want to thank Dr. Alok Pawasker (SSGCH) and Dr. Sameer Joshi (N.M. & MIC) for their suggestions and assistance in finding data sources through various gazettes of hospital resources.

Conflict of interest. None

REFERENCES

Al-Shakhrah, I. I. (2010). A Comparison Between the Values of Renal Parenchymal Mean Transit Time by Applying Two Methods, Matrix Inversion Deconvolution And, Rutland-Patlak Plot. *World Applied Sciences Journal*, *8*(10), 1211–1219.

Andrew, T., Brandon, D., Palma, D., Blaufox, D., Durand, E., Belkis, E., Grant, S., Andrew, J. (2018). SNMMI Procedure Standard/EANM Practice Guideline for Diuretic Renal Scintigraphy in Adults With Suspected Upper Urinary Tract Obstruction 1.0, *Seminars in Nuclear Medicine, 48*(4), 377-390.

ACR Guidelines and Standards Committees (2008). Nuclear Medicine & Pediatric Radiology, ACR Resolution 12, Practice Guideline for the Performance of Adult and Pediatric Renal Scintigraphy.

Blaufox, M., Palma D., Taylor A., Szabo Z., Prigent A., and Samal. M. (2018). The SNMMI and EANM practice guideline for renal scintigraphy in adults. *European Journal of Nuclear Medicine and Molecular Imaging*, *45*, 2218-28

Blum, E. S., Porras, A. R., Biggs, E., Tabrizi P. R., Rachael, D. S., Sprague, B. M., Rana, E. S., Majd, M., Pohl, H. G., Linguraru, M. G. (2018). Early Detection of Ureteropelvic Junction Obstruction Using Signal Analysis and Machine Learning: A Dynamic Solution to a Dynamic Problem. *Journal of Urology*, *199*(3), 847–852.

Dobbeleir, A. A., Piepsz, A., & Ham, H. R. (2008). Pixel-by-pixel mean transit time without deconvolution. *Nuclear medicine communications*, *29*(4), 345-348.

Eoran, B. (1988). The Fast Fourier Transform and its Applications, *Prentice-Hall, Englewood Cliffs, New Jersey.*

Filipczak, K.G., Cichocki, P., Kusmierek, J., Plachcinska, A. (2020). Kidney Efficiency Index-Quantitative parameter of a dynamic renal scintigraphy. I. Theory and preliminary verification. *Nucl. Med. Review*, *23*, 78-83.

Gokhale, P. N., and Patil, B.R. (2022). Correlation Between Renal Tracer Parameters Derived for Recognition of Renal Obstruction with ^{99m}Tc-DTPA Scintigraphy. *In 2022 10th International Conference on Emerging Trends in Engineering and Technology-Signal and Information Processing (ICETET-SIP-22), IEEE*, 1-6.

Gonzalez, R. C. (2001). Digital Image Processing, Ed. 3rd, *Pearson's International*, 320-532.

Gordon, I., Piepsz, A. and Sixt, R. (2011). Guidelines for standard and diuretic renogram in Children, *European Journal of Nuclear Medicine and Molecular Imaging*, *38*(6), 1175-88.

Jagtap, V. (2010). Fast Fourier Transform Using Parallel Processing for Medical Applications, *MSc Thesis, Biomedical Engineering, University of Akron Ohio*.

Jianhua, L. and Yanling, S. (2011). Image Feature Extraction Method Based on Shape Characteristics and Its Application in Medical Image Analysis, *CCIS 224*, 172–178.

Mititelu, R., and Bratu, O. (2017). Radionuclide Imaging. An Update on the Use of Dynamic Renal Scintigraphy: Review. *Modern Medicine*, *24*(4), 199-203.

Patrick, J. V. (1990). Discrete Wavelet Transformations, 2nd Edition.

Suapang, P., Dejhan, K. and Yimman, S. (2015). The estimation of GFR and ERPF using adaptive edge-based active contour for the segmentation of structures in dynamic renal scintigraphy. *International Journal of Innovative Computing, Information and Control*, *11*(1), 87–103.

Tseng, T. Y. and Stoller, M. L. (2009). Obstructive Uropathy. *Clinics in Geriatric Medicine*, *25*, 437–443.

How to cite this article: Gokhale P.N.., Patil B.R.., Joshi Sameer. (2023). Quantitative Measurement and Analysis of Renal Obstruction Using ROI Detection Techniques, *Biological Forum – An International Journal*, *15*(6): 761-767.